Proceedings of IMECE 2006
ASME 2006 International Mechanical Engineering Congress & Exposition
November 05-10, 2006, Chicago, USA

IMECE2006-15957 DRAFT

STATIC AND DYNAMIC MORPHING CHARACTERISTICS OF A CHIRAL CORE AIRFOIL

Alessandro Spadoni
Georgia Institute of Technology
School of Aerospace Engineering
Atlanta, Georgia 30332
Email: alessandro@gatech.edu

Massimo Ruzzene*
School of Aerospace Engineering
Georgia Institute of Technology
Atlanta, Georgia, 30332
Email: massimo.ruzzene@ae.gatech.edu

ABSTRACT

Aeroelastic tailoring requires structural compliance and thus often conflicts with stiffness requirements to carry prescribed aerodynamic loads. Recently however, the application of cellular structural concepts has suggested the potential to achieve compliance while conserving required load-carrying capacity. Among the proposed concepts, a chiral geometry in particular is a novel configuration which features an in-plane negative Poisson's ratio which leads to a very high shear modulus, while maintaining some degree of compliance. In particular, the chiral geometry allows large continuous deformations of the airfoil assembly, with the constitutive material remaining in the linear region of its stress-strain curve. The ability to sustain large deformations without exceeding yield conditions is required to recover the original shape and to provide smooth deformations as required by aerodynamic considerations. In previous work, a coupled-physics model, comprising of simultaneous CFD and elastic analyses, is developed to investigate the influence of the chiral core geometry on the behavior of a given airfoil. The modification of geometric parameters defining the considered layout leads to significant variations in mechanical properties, which can be exploited to achieve various levels of compliance. The morphing capabilities of the proposed airfoil, quantified as camber changes, are evaluated for various design configurations of the internal core structure. Specifically, three such airfoils have been constructed to study the influence of core geometric parameters on the elastic behavior observed in numerical simulations. Experiments on the aforementioned airfoil samples are characterized by imposing large camber-wise deflections, via static loading, and measuring the resulting strain, both in the honeycomb core and in the airfoil profile. The experimental results confirm the ability of the airfoils to sustain large deflections while not exceeding yield strain limits, in addition to producing continuous deformations, which are critical for the implementation of aeroelastic tailoring.

INTRODUCTION

Since the first attempts of powered flight, biologically inspired researchers have tried to devise techniques to implement aeroelastic tailoring as a form of flight control. Albeit few exceptions such as the Wright Flyer and more recent experimental aircraft, aeroelastic tailoring has proven elusive [1]. Aeroelastic tailoring requires structural compliance and thus often conflicts with stiffness requirements to carry prescribed aerodynamic loads. Recently however, the introduction of smart materials and structures, such as composite materials, has encouraged engineers and researches to revisit aeroelastic tailoring, as it promises higher authority and efficiency over current flow control mechanisms. To this day various configurations have been proposed. Among others,

Among other forms of innovative smart structures, cellular solids have been suggested for the design of structural components with superior mechanical properties and multifunctional characteristics. The chiral geometry [2] in particular is a novel configuration which features an in-plane negative Poisson's ra-

*Address all correspondence to this author.

tio which leads to a very high shear modulus, while maintaining some degree of compliance. This unique mechanical behavior can be exploited for the design of sandwich structures with a core composed of a macroscopic chiral truss, laid out across the thickness. This concept, also denoted as "truss-core," lends itself for the design of airfoils with morphing capabilities. In particular, the chiral honeycomb allows for large continuous deformations of the airfoil assembly, while remaining in the linear region of the stress-strain relationship. The ability to sustain large deformations without exceeding yield conditions is required to achieve repeatability, while smooth deformations are imperative for aerodynamic applications such as aeroelastic tailoring. In previous work [3], a coupled-physics model, comprising of simultaneous CFD and elastic analyses, was developed to investigate the influence of the chiral core on the static aeroelastic behavior of a given airfoil. The alteration of geometric parameters defining such layout leads to significant variations in mechanical properties, which can be exploited to achieve different functionalities. The morphing capabilities of the proposed airfoil, here quantified as camber changes, are evaluated for various design configurations of the core. Specifically, three such airfoils have been constructed to study the influence of honeycomb core geometric parameters and relative density on the elastic behavior observed in numerical simulations. In particular, the chiral honeycomb is defined by circular elements acting as nodes, connected by ribs or ligaments tangent to the nodes. Experiments on the aformentioned airfoil samples are characterized by imposing large camber-wise deflections, via static loading, and measuring the resulting strain, both the in the honeycomb core and the airfoil profile. Finally, experimental results confirm the ability of chiral-core airfoils to sustain large deflections while not exceeding yield strain limits, in addition to producing continuous deformations, which are critical for the implementation of aeroelastic tailoring.

CONSIDERED CONFIGURATIONS

The design of deformable systems may be driven by kinematic or mechanic considerations, according to the manner in which the system's deformations take place. Deformations may be desired to alleviate structural forces, they may be passive in nature and arise from low structural stiffness, or they may be actively induced, as in the case of structural mechanisms. Often, the ability of a structural system to deform is coupled with strength requirements, as in the case of multifunctional structural components. Coupled deformability-stiffness requirements arise often in applications for which weight considerations drive the design. Aircraft are a prime example of such requirements.

Given the current state of the art in aerospace design, it is common practice to select an aircraft configuration based on the most frequent conditions encountered during a given mission. for a passenger aircraft, for example, cruise conditions dictate the design. The lifting surfaces of such aircraft, as an example, are optimized to produce the highest lift-to-drag ratio (L/D) at cruise conditions; however, they need to operate properly even for off-design conditions. Such requirements are satisfied by wing reconfiguration, which is often justified in terms of efficiency, while it is in fact required to sustain flight. The deformations to which lifting surfaces are subjected can be divided into passive, due to aeroelastic phenomena, and active, due to the actuation of mechanisms for reconfiguration, such as flaps and slats. Within the realm of passive deformations, elastic deformations may be further differentiated into span-wise and chord-wise directions. Span-wise deformations are in turn characterized by torsional, bending and shearing phenomena. Span-wise bending is usually sought to relieve wing-root stresses, while span-wise torsion is to be avoided as it is one of the major causes of aeroelastic divergence, aileron reversal and flutter [1]. Chord-wise elastic deformations, on the other hand, are currently avoided as they alter wing-section aerodynamic characteristics, and, more importantly, alter the span-wise characteristics of a wing [1, 4], while highly coupling the design of reconfiguration mechanisms with elastic phenomena. Currently employed wings, hence, are highly anisotropic components.

The multifunctionality of wings may be improved if elastic deformations could be exploited as a means to achieve aeroelastic tailoring [1], yielding complexity and weight reduction. To this end, Anisotropy may be exploited to satisfy often conflicting requirements. The aim of the current work, then, is to present a novel wing-section assembly that exploits the exotic mechanic characteristics of the chiral honeycomb [2] to achieve chord-wise deformations, useful for wing-reconfiguration purposes, while possessing high torsional rigidity, paramount to avoiding divergence and flutter.

Airfoil core layout

The novel geometry defining the airfoil core is that of the chiral honeycomb. The geometry of such layout is shown in Fig. 1, where the geometric parameters L, R, r, t, β and θ are also presented. The relation between the aformentioned geometric parameters is suggested by [2], and is defined as follows:

$$tan(\beta) = \frac{2r}{L} \tag{1}$$

$$sin(\beta) = \frac{2r}{R} \tag{2}$$

$$sin(\theta) = \frac{R}{R/2} \tag{3}$$

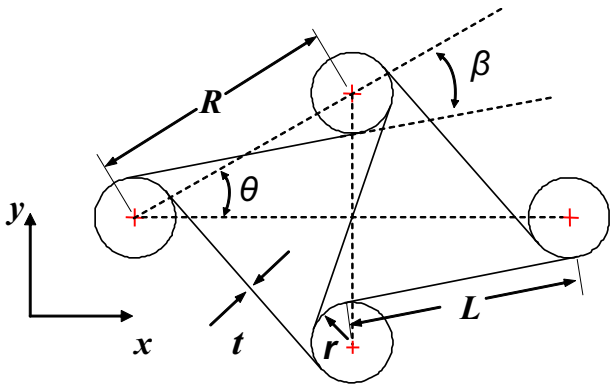

Figure 1. CHIRAL CELL GEOMETRY.

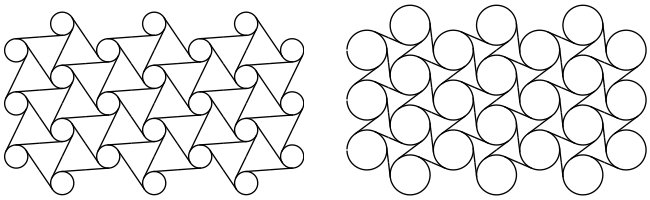

(a) $L/R = 0.90$ (b) $L/R = 0.60$

Figure 2. CHIRAL HONEYCOMB.

while t represents the wall thickness. The resulting lattice defined by chiral geometry is shown in Fig. 2.

Both experimental and analytical results suggest that the chiral honeycomb possesses an in-plane Poisson's ratio, ν of -1, which is the result of a peculiar deformation mechanism characterized by the winding of the ligaments (walls connecting tangent to the circles or nodes) onto the nodes [2]. The obvious consequence of a negative in-plane Poisson's ratio is a high in-plane shear modulus, G, which guarantees in-plane torsional rigidity, necessary to mitigate divergence and flutter. A high shear modulus, furthermore, minimizes in-plane shear deformations, which would alter the airfoil thickness. An additional property of the chiral honeycomb is the ability to sustain large in-plane deformations while being able to recover fully its original dimensions following strains of up to 25 %. This results in a displacement of adjacent nodes along the direction of R [2]. Finally, out-of-plane properties are characterized by a higher compression strength relatively to hexagonal honeycombs [5], which be may exploited to determine span-wise bending stiffness.

Airfoil Characteristics

The ability of the chiral honeycomb to sustain large in-plane deformations, while possessing a large in-plane shear modulus,

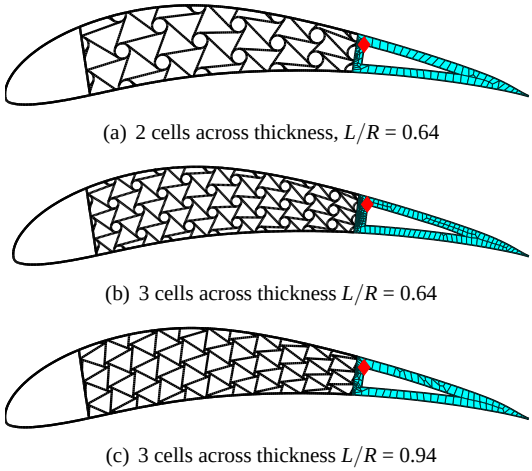

(a) 2 cells across thickness, $L/R = 0.64$

(b) 3 cells across thickness $L/R = 0.64$

(c) 3 cells across thickness $L/R = 0.94$

Figure 3. CHIRAL-CORE AIRFOILS.

offers the opportunity to design highly anisotropic wing profiles, whose in-plane shear deformations are minimized, while favoring chord-wise bending. In previous work [3], the chiral lattice shown in Fig. 2 was accommodated with the airfoil profile. While large chord-wise deformations were obtained within the elastic range of the constitutive material, it was difficult to compare assemblies defined by different geometric parameters, due to the complex interaction of the chiral lattice with the airfoil profile. In the same work [3], a new core configuration is proposed, where the location of the node centers is mapped to adhere to the chosen airfoil profile. The ligaments are then placed tangent to the nodes, yielding the chiral-core airfoils shown in Fig. 3. In this manner the periodicity of the core is lost, but the peculiar deformation mechanism of the chiral honeycomb is retained.

Varying the geometric parameters defining the chiral honeycomb produces the particular configurations shown in Fig. 2. In the current work, in particular, the ratio L/R is varied, as it was shown in [3] that doing so allows the tuning of the chiral behavior to different requirements. In particular, a low L/R ratio promotes the aforementioned winding core deformation mechanism responsible for high airfoil compliance. In the opposite scenario, that is for a high L/R ratio, the characteristic non-centrosymmetric chiral layout, responsible for the negative Poisson's ratio [6] is nearly eliminated, yielding a much stiffer airfoil configuration. In addition to varying the geometry of the airfoil core, the effect of core relative density was also investigated in [3]. This was done by varying the number of chiral unit cells defining the airfoil core. The experimental investigations presented in the current work, consequently, include such scenario as well.

Given the ability of the proposed airfoil core to carry significant in-plane shear loads, and its compliance in in-plane bending, the chord-wise deformations are here quantified in terms of

variations in airfoil mean camber, or in other words decambering effects. For this reason, a highly cambered wing-section, Eppler 420, is chosen as the baseline airfoil configuration. Static aeroelastic simulations presented in [3], in fact, demonstrated the decrease in mean camber line for the chiral-honeycomb core Eppler 420, as a result of increasing free-stream velocity. Such aeroelastic behavior resulted in a quasi-linear relationship between sectional lift, l, and free-stream velocity, V. The aim of the current work, then, is to experimentally validate the findings presented in [3].

NUMERICAL AND EXPERIMENTAL PROCEDURES

The specifical airfoils shown in Fig. 3 have been fabricated with the intent of validating the numerical results presented in [3]. The fabricated airfoils represent a selection of the configurations investigated. Structural numerical models, thus, are included in the current work and compared to experimental results in an effort to obtain a reliable numerical model to be used for further investigations, such as the dynamic response. Numerical models, furthermore, are used to validate and investigate the strain resulting from large chord-wise deformations. Finally, the constitutive material for all considered assemblies is Aluminum with density, $\rho = 2700\ Kg/m^3$, Poisson's ratio, $\nu = 0.33$ and Young's Modulus, $E = 69\ GPa$. The out-of-plane thickness of the airfoil assemblies is 2.54 *cm*, while the airfoil skin and chiral core wall thickness, t, is 0.76 *mm*. All three manufactured airfoil configurations have a chord of 0.7 *m* and a maximum thickness of 8.7 *cm*. Such dimensions where chosen due to manufacturing constraints imposed by the workable are of the OMAX® 2562 Jetmanufacturing® machine.

Numerical Model.

The static equilibrium and dynamic response of the proposed airfoil configurations is predicted by a two-dimensional, linear finite-element (FE) model, whereby beam and plane elements are used to discretize the structural system. In particular, both beam an planar elements are used, as the chiral honeycomb occupies only part of the wing profile (Fig. 3). The airfoil profile and chiral core are hence analyzed as a frame structure, with beam elements featuring both axial and transverse degrees of freedom. Transverse shear deformations are included according to the formulation presented in [7], in order to avoid inaccuracies derived from the presence of non-slender elements. Classical isoparametric planar elements are employed to model the trailing edge region, where it is assumed that a homogeneous material is utilized. The mesh employed for such regions includes both triangular and quadrilateral elements. The quadrilateral elements are of the bilinear kind, developed according to the formulation denoted as Q6 in [7]. The planar triangular elements used are constant strain elements. Both triangular and quadrilateral elements feature drilling DOFs, which allow their coupling with the beam elements used for chiral structure and skin discretization.

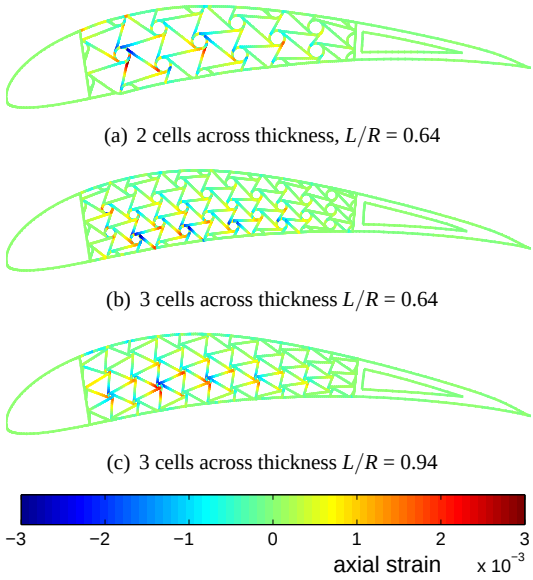

Figure 4. NUMERICALLY-PREDICTED STRAIN DISTRIBUTION DUE TO A CONCENTRATED LOAD.

Core is very complicated, hence linear analisys is good.

Fabrication Process and Experimental Set-Up.

Fabrication of the chiral-core airfoils has been realized with a OMAX® 2562 Jetmanufacturing® machine. The airfoil assemblies were cut out of an unstressed Aluminum plate of thickness 2.54 *cm*. The aluminum grade is T6051.

Static Experimental Set-Up. In order to validate the ability of the chiral core to sustain large deformations and remain with the elastic range of the constitutive material, the leading edge is clamped, while the trailing edge is loaded by a concentrated load, in the location indicated by the red diamond in Fig. 3. The concentrated load is applied in the direction of the airfoil thickness. The strain in the core of the airfoil profile is monitored in 6 different locations by single-element strain gages. Furthermore, the displacement of the trailing edge is monitored by a LVDT displacement transducer.

EXPERIMENTAL AND NUMERICAL RESULTS

The locations where the strain gages are placed have been chosen based on a linear finite-element model. The strain distribution within the core and airfoil profile, for the three configurations fabricated, is shown in Fig. 4. Such strain distribution is the result on an applied concentrated load at the trailing-edge

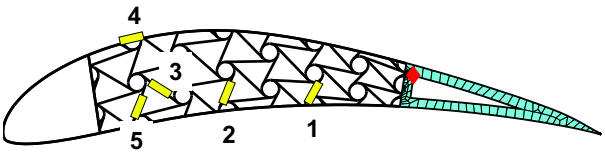

Figure 5. STRAIN GAGE LOCATIONS FOR THE AIRFOIL CONFIGURATION DEFINED BY 2 CELLS ACROSS THE AIRFOIL THICKNESS AND L/R = 0.64.

location shown in Fig. 3, indicated by a diamond, whith the leading edge region clamped. In the case of the airfoil core defined by 2 unit cells across the airfoil thickness and a ratio of L/R = 0.64 (see Fig. 3a), the strain distribution in shown in Fig. 4a. The corresponding strain gage locations are shown in Fig. 5. A load hysteresis is carried out based on the results from the numerical model. For the case of 2 cells across the thickness and L/R = 0.64, such models indicate the assembly is capable of carrying up to 19.6 N while in the elastic range of the constitutive material. A hysteresis load schedule of up to 19.6 N, on the other hand, produced the strain and trailing edge displacement history shown in Fig. 6. All strain gages, as well as the trailing edge displacement, show a residual deformation at the completion of the loading schedule. The reason for the use of a linear finite-element model to predict strain is based on the complexity of the airfoil core, which, even for large decambering deformations, is expected the present much smaller local displacements. In the case of the airfoil configuration shown in Fig. 5, however, the airfoil-core relative density is much lower than that of the other considered configurations. This may possibly have caused the linear finite-element model to underpredict the strain with the core.

The strain distribution, due to the aformentioned applied concentrated load, within the core and airfoil profile, for the airfoil configuration denfined by 3 unit cells across the thickness and a ratio l/R = 0.60, is shown in Fig. 4b. The corresponding strain gage locations are shown in Fig. 7. Once again, a load hysteresis is carried out based on the results from the corresponding numerical model. For the case of 3 cells across the thickness and L/R = 0.60, the finite-element model indicates the assembly is capable of carrying up to at least 72.5 N while in the elastic range of the constitutive material. A hysteresis load schedule of up to 72.5 N produced the strain and trailing edge displacement history shown in Fig. 8. All strain gages, as well as the trailing edge displacement, show no residual deformation at the completion of the loading schedule. The absence of residual deformations the the end of the load hysteresis thus confirms the finite-element model predictions, which appear to be more accurate since the airfoil-core relative density is much higher than that of the configuration defined by 2 unit cells across the airfoil

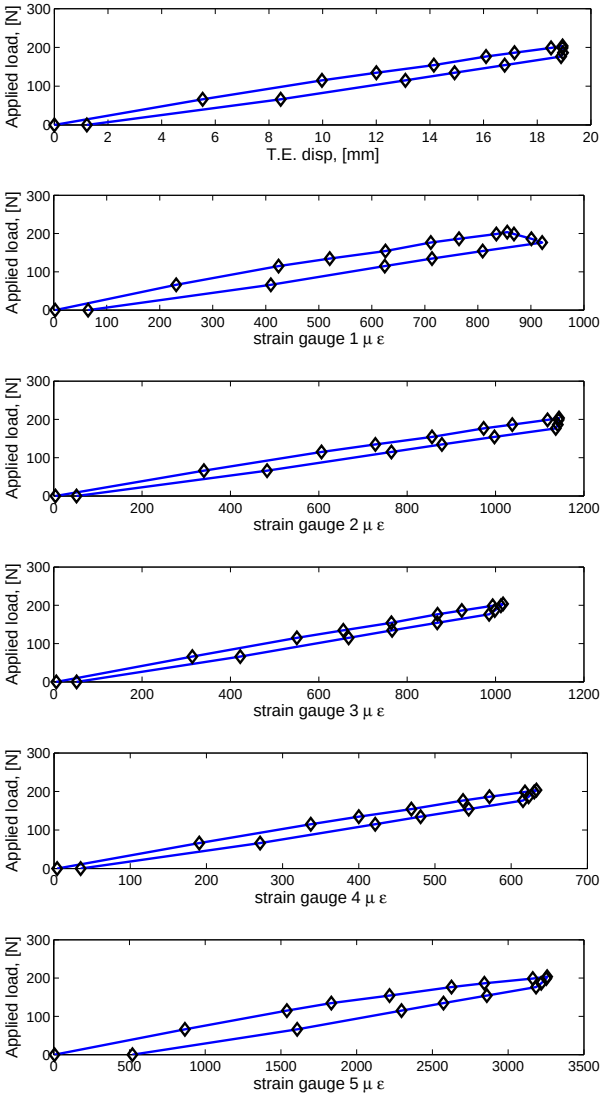

Figure 6. STRAIN RESPONSE AND TRAILING EDGE DISPLACEMENT FOR THE AIRFOIL CONFIGURATION DEFINED BY 2 CELLS ACROSS THE AIRFOIL THICKNESS AND L/R = 0.64.

thickness.

The strain distribution, due to the aformentioned applied concentrated load, within the core and airfoil profile, for the airfoil configuration denfined by 3 unit cells across the thickness and a ratio l/R = 0.94, is shown in Fig. 4c. The corresponding strain gage locations are shown in Fig. 9. Similarly to the previous cases, a load hysteresis is carried out based on the results from the corresponding numerical model. For the case of 3 cells across the thickness and L/R = 0.94, the corresponding finite-element model indicates the assembly is capable of carrying up to at least 90.4 N while in the elastic range of the constitutive ma-

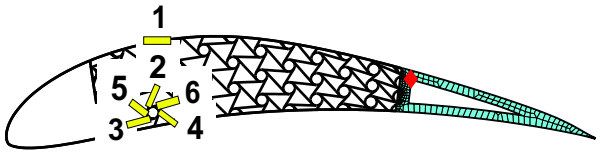

Figure 7. STRAIN GAGE LOCATIONS FOR THE AIRFOIL CONFIGURATION DEFINED BY 3 CELLS ACROSS THE AIRFOIL THICKNESS AND L/R = 0.60.

terial. A hysteresis load schedule of up to 90.4 N produced the strain and trailing edge displacement history shown in Fig. 10. All strain gages, as well as the trailing edge displacement, show no residual deformation at the completion of the loading schedule. The absence of residual deformations the the end of the load hysteresis thus confirms the finite-element model predictions.

The discrepancy of predicted strain levels by the corresponding finite-element models, for each of the three manufactured airfoils, with experimentally recorded strain can be attributed to at least two factors. Firstly, the linear finite-element model for the core configuration defined by 3 unit cells across the airfoil thickness and L/R = 0.64 proved inadequate, as such airfoil possesses a deformation mechanism whereby large decambering deformations are associated with large airfoil core displacements, possibly due to low relative density. A second factor influencing the experimentally recorded strain is the chiral honeycomb deformation mechanism, and the placement of strain gages. In particular, previous work [2] demonstrated that, for small displacements, the chiral honeycomb produces the characteristic deformed configuration shown in Fig. 11. A simple free-body diagram of ligament tangent to the nodes produces an structural element loaded by two concentrated moments at the element's extremities [2]. If such ligament is treated as a slender beam, for which Euler-Bernoulli beam theory can be applied, the corresponding strain distribution is linearly varying from maximum values at the ligament's ends [8]. Not all airfoil core configurations, however, permitted the placement of strain gages at the ligament's ends. For high relative-density configurations such as the one defined by 3 cells across the airfoil thickness and L/R = 0.64 in particular, at least three strain gages were placed near the middle of the chosen ligaments. Referring to Fig. 8, strain gages corresponding to locations 1,4 and 6 (see also Fig. 7) produced strain values not inline with those of locations 2 and 5, in disagreement with numerical models. Nonetheless, the absence of residual deformations can be assessed, even with strain gages placed away from maximum strain areas.

SUMMARY

The ability of chiral honeycomb to sustain large deformations while remaining in the elastic range of the constitutive material has been assessed. In the current work in particular, a novel wing-section configuration is proposed as a away to exploit the mechanic capabilities of the chiral honeycomb. Three airfoils with honeycomb truss core have been manufactured and tested to validate the predictions of numerical, linear finite-element models. It is found that configurations characterized by the complex honeycomb core ,albeit with low relative density, require the use or large-deformation numerical models. If core relative density is not low, on the other hand, linear finite-element models prove accurate. The assemblies characterized by 3 honeycomb unit cells across the thickness demonstrated their ability to sustain large decambering deformations, while their core remains within the elastic region of the constitutive material. Refined numerical models, however, are needed to comfortably predict the behavior of chiral-core airfoil assemblies, and such is the aim of future work.

ACKNOWLEDGMENT

Thanks go to D. E. Knuth and L. Lamport for developing the wonderful word processing software packages TEX and LATEX. I also would like to thank Ken Sprott, Kirk van Katwyk, and Matt Campbell for fixing bugs in the ASME style file `asme2e.cls`, and Geoff Shiflett for creating ASME bibliography stype file `asmems4.bst`.

REFERENCES

[1] Hodges, D., and Pierce, G., 202. *Introduction to Structural Dynamics and Aeroelasticity*. Cambridge University Press, New York, NY.

[2] Prall, D., and Lakes, R., 1997. "Properties of a chiral honeycomb with a poisson's ratio of -1". *International Journal of Mechanical Sciences*, **39**(3), pp. 305 – 14.

[3] Spadoni, A., and Ruzzene, M., 2005. "Static aeroelastic behavior of a chiral-core airfoil". *Proceedings of ICAST - Sixteenth International Conference on adaptive Structures and Technologies*, **1**(1), pp. 190 – 198.

[4] Ghiringhelli, G., and Mantegazza, P., 1994//. "Linear, straight and untwisted anisotropic beam section properties from solid finite elements". *Composites Engineering*, **4**(12), pp. 1225 – 39.

[5] Spadoni, A., Ruzzene, M., and Scarpa, F., 2005. "Global and local linear buckling behavior of a chiral cellular structure". *Physica Status Solidi B*, **242**(3), pp. 695 – 709.

[6] Lakes, R., 1991. "Deformation mechanisms in negative poisson's ratio materials: structural aspects". *Journal of Materials Science*, **26**(9), pp. 2287 – 92.

[7] R. Cook, S. Malkus, D. P., and Witt, D., 2001. *Concepts and Applications of Finite Element Analysis*. Fourth Edition, Wiley, New York, NY.

[8] Gere, J., 2001. *Mechanics of Materials*. Brooks/Cole, New York, NY.

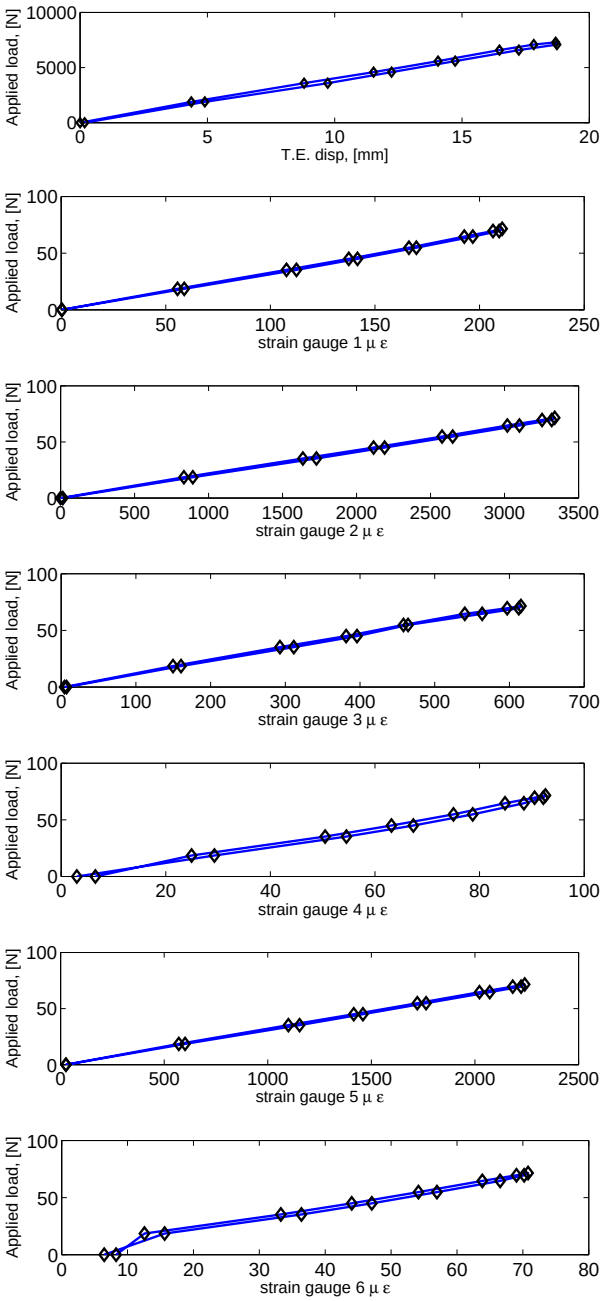

Figure 8. STRAIN RESPONSE AND TRAILING EDGE DISPLACEMENT FOR THE AIRFOIL CONFIGURATION DEFINED BY 3 CELLS ACROSS THE AIRFOIL THICKNESS AND L/R = 0.60.

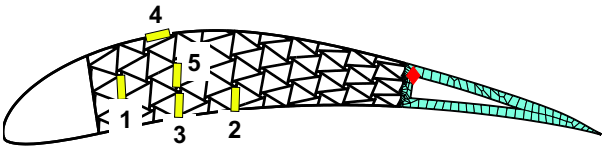

Figure 9. STRAIN GAGE LOCATIONS FOR THE AIRFOIL CONFIGURATION DEFINED BY 3 CELLS ACROSS THE AIRFOIL THICKNESS AND L/R = 0.94.

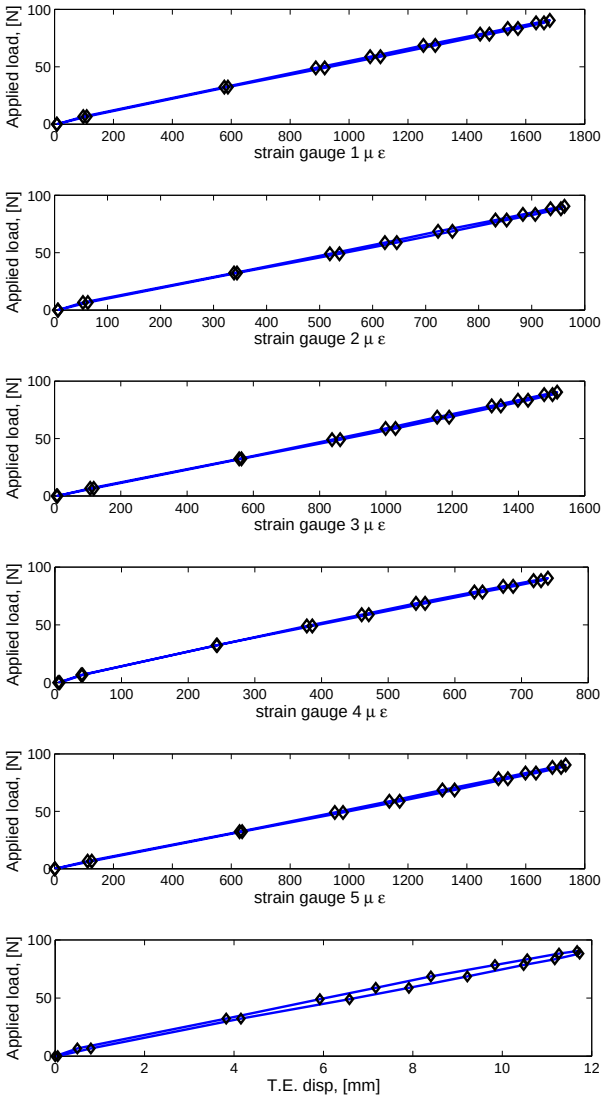

Figure 10. STRAIN RESPONSE AND TRAILING EDGE DISPLACEMENT FOR THE AIRFOIL CONFIGURATION DEFINED BY 3 CELLS ACROSS THE AIRFOIL THICKNESS AND L/R = 0.94.

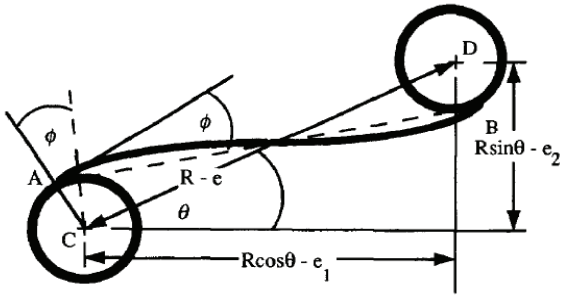

Figure 11. CHIRAL DEFORMATION MECHANISM [2].